International Communications in Heat and Mass Transfer 37 (2010) 914–923

Contents lists available at ScienceDirect

International Communications in Heat and Mass Transfer

journal homepage: www.elsevier.com/locate/ichmt

Microwave pre-curing of natural rubber-compounding using a rectangular wave guide ☆

Natt Makul, Phadungsak Rattanadecho *

Research Center for Microwave Utilization in Engineering (R.C.M.E.), Department of Mechanical Engineering, Faculty of Engineering, Thammasat University, (Rangsit Campus), Khlong Luang, Prathum thani, 12121, Thailand

ARTICLE INFO

Available online 15 April 2010

Keywords:
Pre-heating
Natural rubber-compounding
Microwave
Rectangular wave guide

ABSTRACT

This article presents a new method to pre-cure natural rubber-compounding (NRc) by using microwave energy at a frequency of 2.45 GHz with a rectangular wave guide. The influences of microwave power input, specimen thicknesses, and vulcanized sulfur contents on the dielectric and thermal characteristics and cross-linked contents of microwave-cured NRc are studied. Furthermore, a generalized mathematical model for predicting temperature distribution inside the specimen during pre-heating is proposed. Significant results show that microwave energy can produce partial cross-linking at temperatures below the actual vulcanizing process. The numerical results from the model agree well with the results from the experiments.

1. Introduction

Most rubber in everyday use is what is known as natural rubber, which is a polymer of isoprene with low elastic properties. Therefore, it is often treated with a vulcanization process; in this process, the rubber is cured by heat and sulfur, peroxide, or bisphenol is added to it in order to improve resilience and elastic properties and to prevent it from perishing. In addition, carbon black is usually used as an additive for improving the rubber's strength by inducing cross-links to form between the polymer chains in order to limit the chain's ability to move independently. At present, most conventional vulcanization processes depend on temperature and sulfur content [1–7]. Nevertheless, large amounts of sulfur together with a high temperature and a long curing period do not bring about satisfactory cross-linking efficiency, a consequence of which is a reduction in the rubber's strength. In addition, various conventional heating methods apply and dissipate heat via the rubber's thermal properties; this is the case even though natural rubber is inherently an insulation material that causes ineffective heat distribution during processing.

Given the advantages of microwave heating, such as short start-up time, cleanness, and high-speed, selective, volumetric heating, it is reasonable to use it to vulcanize rubber. Microwave heating can be used in (a) pre-heating of NRc prior to product casting, (b) rapid curing in a primary process stage, and (c) drying as a secondary post-curing stage. These may be required individually or in combinations that are either applied sequentially or with some overlap.

Research has explored many of the processes involved in curing rubber. The areas covered include the separation of tires becoming to carbon [8]; the chemical disintegration of vulcanized reclaimed rubber [9]; the dielectric properties of natural rubber before and after vulcanizing [10]; the cross-linking of rubber in microwave curing processes [11]; the vulcanization of elastomers [12]; and microwave-assisted cross-linking carried out in relation to microwave tunnels [13]. In terms of the experimental investigations into the use of microwave energy to assist with the vulcanization process, many studies have developed mathematical models to gain insight into the related phenomena taking place within the wave guide together with the temperature distribution in the NRc specimen to be processed. In particular, two-dimensional models of the interactions between electromagnetic (microwave) fields and dielectric materials in a variety of microwave applicator configurations such as rectangular wave guides and cavities have been studied [14–16].

Although most of the previous investigations experimented with the simulation points of rubber during microwave curing, little work has been published on microwave curing of rubber in a rectangular wave guide. In particular, full comparison between mathematical simulations is taken into account. Therefore, this work carries out experimental microwave pre-curing of NRc by transmitting energy with a rectangular wave guide and a microwave in TE_{10} mode with a frequency of 2.45 GHz. In addition the temperature increase during microwave heating is also simulated numerically and then validated with the experimental results. The results presented here provide a basis for developing a fundamental understanding of pre-curing NRc using microwave energy.

2. Experiments

2.1. Dielectric properties measurement

The open-ended probe technique was employed for measuring the dielectric properties of NRc. This technique, by itself, calculated the dielectric properties from the phase and amplitude of the reflected

☆ Communicated by W.J. Minkowycz.
* Corresponding author.
E-mail address: ratphadu@engr.tu.ac.th (P. Rattanadecho).

0735-1933/$ – see front matter © 2010 Elsevier Ltd. All rights reserved.
doi:10.1016/j.icheatmasstransfer.2010.03.001

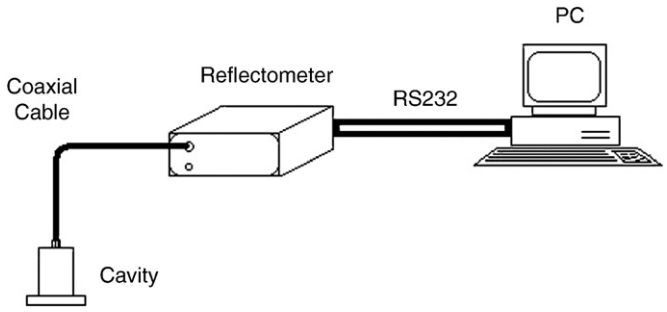

Fig. 1. Portable network analyzer.

signal at the end of an open-ended coaxial line, which was inserted into a specimen measured by a portable network analyzer, as shown Fig. 1. The analyzer consists of a coaxial cavity, microwave reflectometer, 0.35-cm coaxial cable, 0.35-cm female calibration, and short- and open-matched load and software. The coaxial cavity is characterized by a measurement range of 1.5–2.6 GHz with a precision of not more than 2% of the dielectric constant and 5% of the dielectric loss factor. The measured specimen should be assumed to be of infinite size and non-magnetic material, and have isotropic and homogeneous properties. In addition, the coaxial cavity must be in close contact to the specimen during the test.

2.2. Microwave process

Fig. 2a shows an experimental apparatus. The microwave system generates a monochromatic wave by magnetron that operates a transverse electric (TE_{10}) mode at a frequency of 2.45 GHz. The microwave is transmitted along the z-direction of the rectangular wave guide with inside dimensions of 10.92 cm × 5.46 cm toward a water load positioned at the end of the wave guide (Fig. 2b). The water load (lower absorbing boundary) ensured that only a minimal amount of the microwave is reflected back to the specimen. The warm water load is circulated through the cooling tower to reduce the temperature in the water load system.

A rectangular-shaped rubber specimen was placed perpendicular to the direction of irradiation via a rectangular wave guide. During

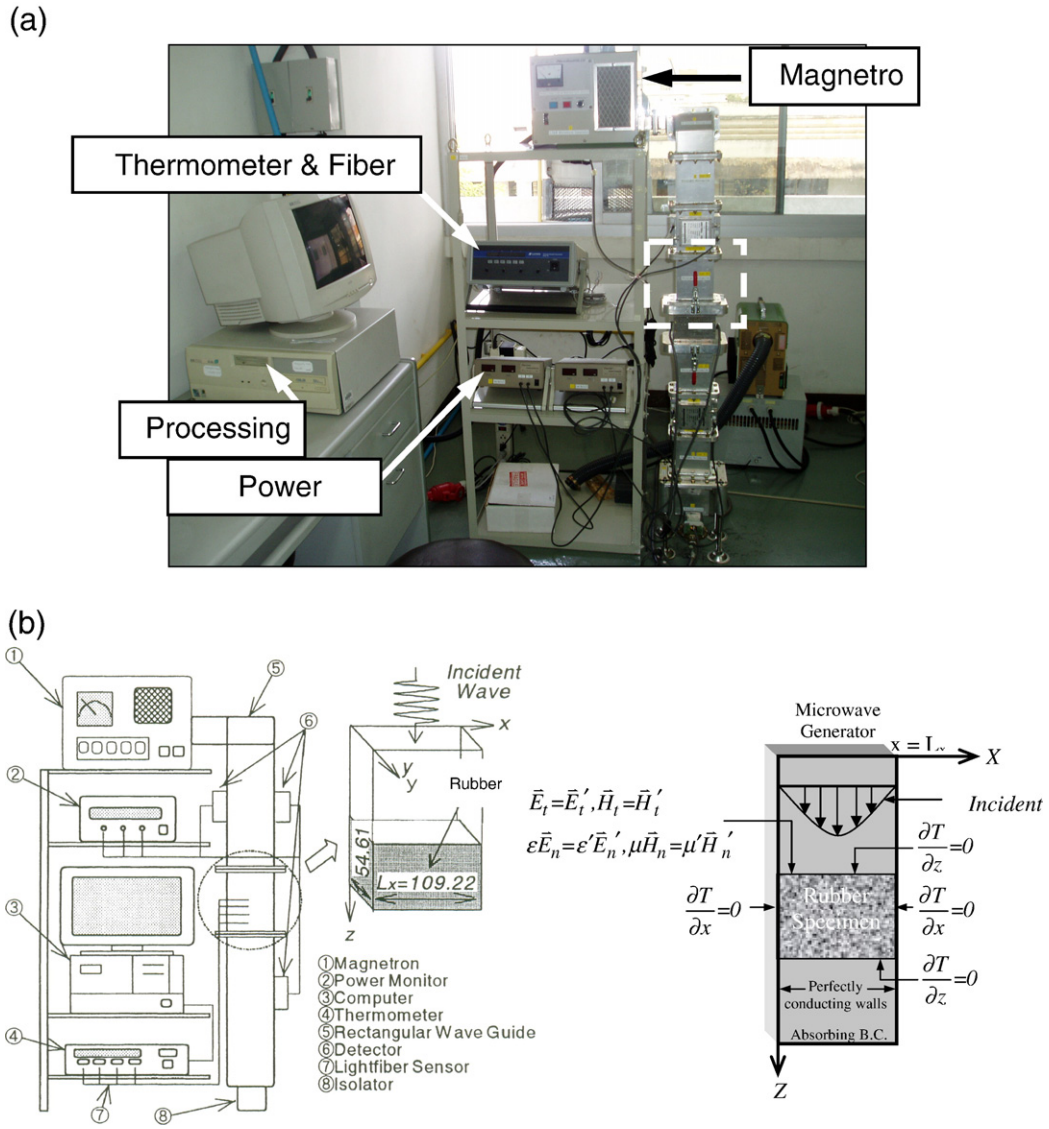

Fig. 2. Microwave heating system with a rectangular wave guide (single-mode applicator): (a) experimental microwave system configuration and (b) physical model.

testing, the output of magnetron was adjusted to the specified power of 1000 W. The powers of incident reflected and transmitted waves with the microwave pre-cured NRc were measured by a wattmeter using a directional coupler. An infrared camera was used to detect the temperature distribution within the processed specimen.

2.3. Specimen preparation

The raw materials consisted of a rubber bar grade STR 20, Dibenzothiazyl disulphide (MBTS) and Diphenyl guanidine (DPG) as activators, sulfur as the vulcanizing agent, and carbon black-grade N 330 as the compounding agent. However, because vulcanizing natural rubber by using sulfur only with no accelerators took several hours and is no longer commercially viable [17,18], here both ZeO and stearic acid act as accelerators. They were proportioned by the weight of the rubber dry, as shown in Table 1. Significantly, their sulfur contents were varied from 1.5 to 2.0, 2.5 and 3.0 parts per hundred parts of dried rubber by weight basis, respectively.

Before mixing, the NRc was classified into two groups, namely (a) NRc without carbon black and (b) NRc with carbon black. As shown in Fig. 3, the NRc in each group was ground by two roll mills at a temperature level of 70 °C for 10 min, referred to as mastication, until its surface becomes soft, with the addition of ZeO and stearic acid, MBTS and PDG with consecutive grinding times of 3, 3, and 15 min, respectively. After that, the first group was continually ground with sulfur until a homogeneous mixture was achieved, while the later group was blended with carbon black for 3–5 min and was then mixed with sulfur. In addition, mixing steps should be limited in duration and uniformity, as longer mixing times effect the production of scorch; this is the onset of curing, whereby chemical reactions begin to occur in the NRc specimen as it was being heated, resulting in rubber losing its ability in processing. After mixing has finished, the NRc was pressed into a mold at a cross-sectional area of 10.7×5.2 cm^2 and thicknesses of 1.0 cm, 2.0 cm, and 3.0 cm.

2.4. Testing procedures

Detailed testing procedures started from testing dielectric properties by preparing an NRc specimen with a diameter of 6.50 cm and a thickness of 1.0 cm and then measuring the NRc by using portable network analyzer. The five values obtained were averaged in order to represent the dielectric properties of each NRc mixture.

To test the chemical properties of the treated NRc after microwave pre-heating, we used cross-linking content and chemical structure as indicators and also compared the chemical properties of an NRc specimen subjected to conventional heating. Normally, the cross-linking is a process of forming a three-dimensional network structure from a linear polymer by a chemical and/or physical method that can be represented by cross-linked content as a percentage. The specimen

Table 1
Mix proportions of NRcs used for studying (unit in phr[a]).

Mix symbol	Raw materials						
	STR 20	ZnO	Stearic aid	MBTS[b]	DPG[c]	Sulfur (S)	Carbon black
NR-S1.5	100	0.5	1.0	0.8	0.2	1.5	0
NR-S2.0	100	0.5	1.0	0.8	0.2	2.0	0
NR-S2.5	100	0.5	1.0	0.8	0.2	2.5	0
NR-S3.0	100	0.5	1.0	0.8	0.2	3.0	0
NRC-S1.5	100	0.5	1.0	0.8	0.2	1.5	10
NRC-S2.0	100	0.5	1.0	0.8	0.2	2.0	10
NRC-S2.5	100	0.5	1.0	0.8	0.2	2.5	10
NRC-S3.0	100	0.5	1.0	0.8	0.2	3.0	10

[a] Part per hundred parts by weight of rubber dry basis (phr).
[b] Dibenzothiazyl disulphide.
[c] Diphenyl guanidine.

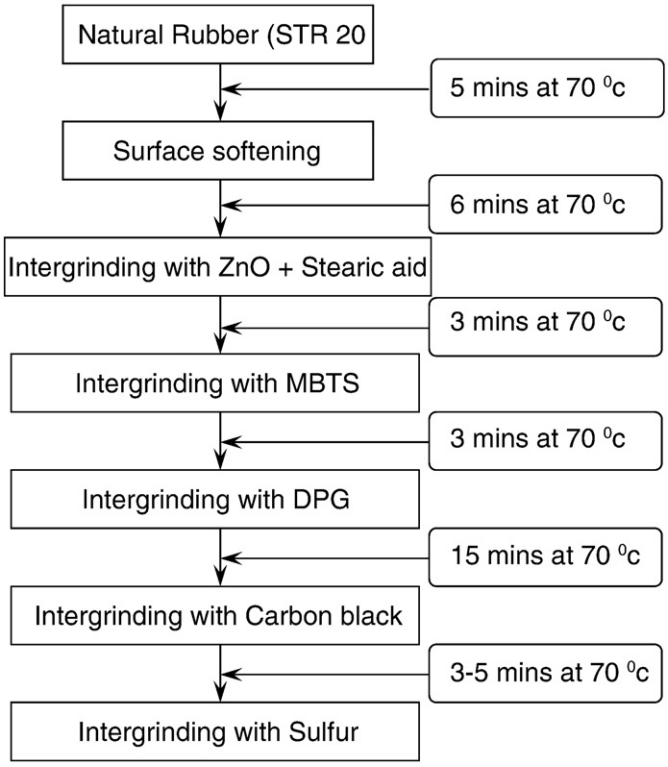

Fig. 3. Procedures for preparing NRc with and without carbon black.

was cut to a rectangular shape and then was weighted both before and after soaking in 30 ml of toluene for 7 days. These weights were used to calculate cross-linked content as shown in Eq. (1) [17,18]. The Fourier Transform Infrared Spectrometer (FTIR) technique was used to identify the chemical structure characteristics of the treated NRc:

$$\eta_{swell} = \frac{-\ln(1-V_r) - V_r - \chi V_r^2}{V_m\left(V_r^{1/3} - \frac{V_r}{2}\right)} \quad (1)$$

where V_r is the volume fraction of rubber in swollen gel, χ is the rubber-solvent interaction parameter (0.406), V_m is the molar volume of toluene (106.8 cm^{-3} mol) and η_{swell} is the swelling of rubber (%).

3. Analysis of microwave heating using a rectangular wave guide

3.1. Electromagnetic simulation

As shown in Fig. 2b, a physical model for the microwave pre-curing of NRc using a rectangular wave guide is proposed. Since microwave radiation in the TE_{10} mode as propagated in the rectangular wave guide is uniform in the y-direction, the electromagnetic field can be considered in a two-dimensional model on the x–z plane. Corresponding to the electromagnetic field, temperature fields also can be considered in the two-dimensional model. The model proposed is based on the following assumptions:

(1) The absorption of the microwave by air in the rectangular wave guide is negligible.
(2) The walls of the rectangular wave guide are perfect conductors.
(3) All NRc materials are non-magnetic.
(4) The effect of the specimen container on the electromagnetic and temperature fields can be neglected.

Assuming the microwave in the TE_{10} mode into Maxwell's equations, the governing equations for the electromagnetic field can be

written in terms of the component notations of the intensities of the electric and magnetic fields [17]:

$$\frac{\partial E_y}{\partial z} = \mu\frac{\partial H_x}{\partial t}, \frac{\partial E_y}{\partial x} = -\mu\frac{\partial H_z}{\partial t}, -\left(\frac{\partial H_z}{\partial x} - \frac{\partial H_x}{\partial z}\right) = \sigma E_y + \varepsilon\frac{\partial E_y}{\partial t} \tag{2}$$

where E and H denote the electric field and magnetic field intensities, respectively. The subscripts of x, y, and z represent x, y, and z components of vectors, respectively. Further, permittivity or dielectric constant ε, magnetic permeability μ, and electric conductivity σ are given by

$$\varepsilon = \varepsilon_0\varepsilon_r, \mu = \mu_0, \sigma = 2\pi f\epsilon\tan\delta \tag{3}$$

In addition, if magnetic effects are negligible, which is true for most dielectric materials used in microwave heating applications, the magnetic permeability (μ) is well approximated by its value μ_0 in the free space. In this study, all dielectric properties are directly taken from reference [17].

Corresponding to the physical model as shown in Fig. 2b, the boundary conditions can be given as follows:

(a) Perfectly conducting boundaries, that is, boundary conditions on the inner wall surface of a rectangular wave guide are given by using Faraday's law and Gauss's theorem:

$$E_t = 0, \quad H_n = 0 \tag{4}$$

(b) Continuity boundary condition, that is, boundary conditions along the interface between different materials, for example between air and dielectric material surfaces, are given by using Ampere's law and Gauss's theorem:

$$E_t = E_t^{'}, H_t = H_t^{'}, D_n = D_n^{'}, B_n = B_n^{'} \tag{5}$$

(c) Absorbing boundary condition, that is, at both ends of the rectangular wave guide, the first-order absorbing conditions are applied:

$$\frac{\partial E_y}{\partial t} = \pm\upsilon\frac{\partial E_y}{\partial z} \tag{6}$$

Here, the symbol $\pm$ represents forward or backward waves, and υ is the phase velocity of the microwave.

(d) Oscillation of the electric and magnetic field intensities by magnetron; that is, the incident wave due to magnetron is given by the following equations [17]:

$$E_y = E_{yin}\sin\left(\frac{\pi x}{L_x}\right)\sin(2\pi ft), H_x = \frac{E_{yin}}{Z_H}\sin\left(\frac{\pi x}{L_x}\right)\sin(2\pi ft) \tag{7}$$

Z_H is the wave impedance defined as

$$Z_H = \frac{\lambda_g Z_I}{\lambda_0} = \frac{\lambda_g}{\lambda_0}\sqrt{\frac{\mu_0}{\varepsilon_0}} \tag{8}$$

3.2. Heat transport simulation

The temperature distribution of NRc when it is exposed to an incident wave is obtained by solving the heat transport equation with the microwave power included as a local electromagnetic heat-generation term [17]:

$$\frac{\partial T}{\partial t} = a\left(\frac{\partial^2 T}{\partial x^2} + \frac{\partial^2 T}{\partial z^2}\right) + \frac{Q}{\rho\cdot C_p} \tag{9}$$

where T is temperature, a is thermal diffusivity, ρ is density, c_p is heat capacity at constant pressure. Q is defined based on the Lambert's law, the microwave energy absorbed can be defined in Eq. (10) [17]:

$$Q = 2\pi f\epsilon_0\epsilon_r^{'}(\tan\delta)E^2 \tag{10}$$

where Q is the microwave energy, σ is the effective conductivity, f is the frequency, ε_0 is the permittivity of free space (8.8514×10^{-12} F/m), $\epsilon_r^{'}$ and $\epsilon_r^{''}$ are the real and imaginary parts, respectively, of the complex permittivity, $\tan\delta$ is the loss tangent coefficient, and E the is electric field intensity.

The initial condition of the multi-layered materials is defined as $T = T_0$ at $t = 0$. The boundary conditions for solving the heat transport equation are shown in Fig. 2.

3.3. Numerical technique

In order to predict the dissipation of electromagnetic field, a finite difference time domain (FDTD) method is applied. In this study, the leapfrog scheme is applied to a set of Maxwell's equations. The electric field vector components are offset one-half cell in the direction of their corresponding components, while the magnetic field vector components are offset one-half cell in each direction orthogonal to their corresponding components. The electric field and magnetic field are evaluated at alternate half-time steps. For the TE_{10} mode, the electric and magnetic field components are expressed by the total field FDTD equations [17] as

$$E_y^n(i,k) = \frac{1-\frac{\sigma(i,k)\Delta t}{2\varepsilon(i,k)}}{1+\frac{\sigma(i,k)\Delta t}{2\varepsilon(i,k)}}E_y^{n-1}(i,k) + \frac{1}{1+\frac{\sigma(i,k)\Delta t}{2\varepsilon(i,k)}}\frac{\Delta t}{\varepsilon(i,k)} \times\left\{\frac{-\left(H_z^{n-1/2}(i+1/2,k)-H_z^{n-1/2}(i-1/2,k)\right)}{\Delta x} + \frac{\left(H_x^{n-1/2}(i,k+1/2)-H_x^{n-1/2}(i,k-1/2)\right)}{\Delta z}\right\} \tag{11}$$

$$H_x^{n+1/2}(i,k+1/2) = H_x^{n-1/2}(i,k+1/2) + \frac{\Delta t}{\mu(i,k+1/2)} \times\left\{\frac{E_y^n(i,k+1)-E_y^n(i,k)}{\Delta z}\right\} \tag{12}$$

$$H_z^{n+1/2}(i+1/2,k) = H_z^{n-1/2}(i+1/2,k) - \frac{\Delta t}{\mu(i+1/2,k)} \times\left\{\frac{E_y^n(i+1,k)-E_y^n(i,k)}{\Delta x}\right\} \tag{13}$$

Further, the heat transport equation (Eq. (14)) is solved by the finite differences method. The spatial and the temporal terms are approximated using finite difference equations for the electromagnetic field and temperature field. As shown spatially in Fig. 4, Eq. (15) and the discretized heat transport equation are solved on this grid system. The choice of spatial and temporal resolution is motivated by reasons of stability and accuracy.

To ensure the stability of the time-stepping algorithm, Δt must be chosen to satisfy the courant stability condition:

$$\Delta t \le \frac{\sqrt{(\Delta x)^2 + (\Delta z)^2}}{\upsilon} \tag{14}$$

and the spatial resolution of each cell is defined as

$$\Delta x, \Delta z \le \frac{\lambda_g}{10\sqrt{\varepsilon_r}} \tag{15}$$

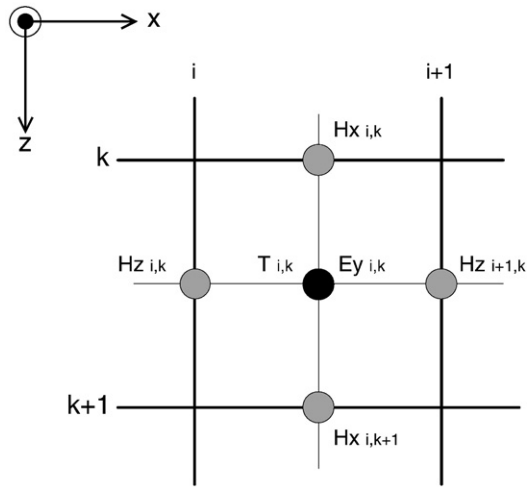

Fig. 4. Grid system configuration.

Corresponding to Eqs. (14) and (15), the calculation conditions are as follows:

(1) To ensure that each wavelength of the microwave in the computational domain for a frequency of 2.45 GHz has more than 10 subdivisions in the numerical calculation, the computational domain is conservatively set, such that the spatial resolution of each cell is $\Delta x = \Delta z \leq \lambda_{mg} / 10\sqrt{\varepsilon_r} \approx 0.1$ cm. Thus, the total of 110×250 cells in the computational domain are used in the numerical calculation.
(2) Because the propagating velocity of the microwave is very fast compared with the rate of heat transfer, the different time steps of $dt = 1$ [ps] and 1[s] are used to compute the electromagnetic field and temperature field, respectively. The spatial step size is $dx = dz = 0.1$ cm.
(3) Relative errors in the iteration procedure of 10^{-8} are chosen.

3.4. Iterative computational schemes

Since the dielectric properties of NRc are temperature-dependent, to understand the influence of the electromagnetic field on microwave heating realistically, it is necessary to consider the coupling between the electric field and the temperature field. For this reason, iterative computational schemes are required to resolve the coupled non-linear Maxwell's equations and heat transport equations.

The computational scheme is to first compute a local heat-generation term by running an electromagnetic calculation with uniform properties, determined from initial temperature data. The electromagnetic calculation is performed until a sufficient period is reached in which a representative average rms (root-mean-square) of the electric field at each spatial point is obtained, typically 30,000 time steps. The microwave power absorption at each point is computed and used to solve the time-dependent temperature field. Using these temperatures, new values for the dielectric properties are calculated and used to recalculate the electromagnetic fields and then microwave power absorption. All the steps are repeated until the required heating time is reached. The details of the computational schemes and strategy are illustrated in Fig. 5.

4. Results and discussion

4.1. Dielectric properties

Table 1 shows the dielectric properties of the NRcs with and without carbon black before pre-heating by microwave energy. It can be seen that the relative dielectric constant ϵ'_r of the NRc specimens

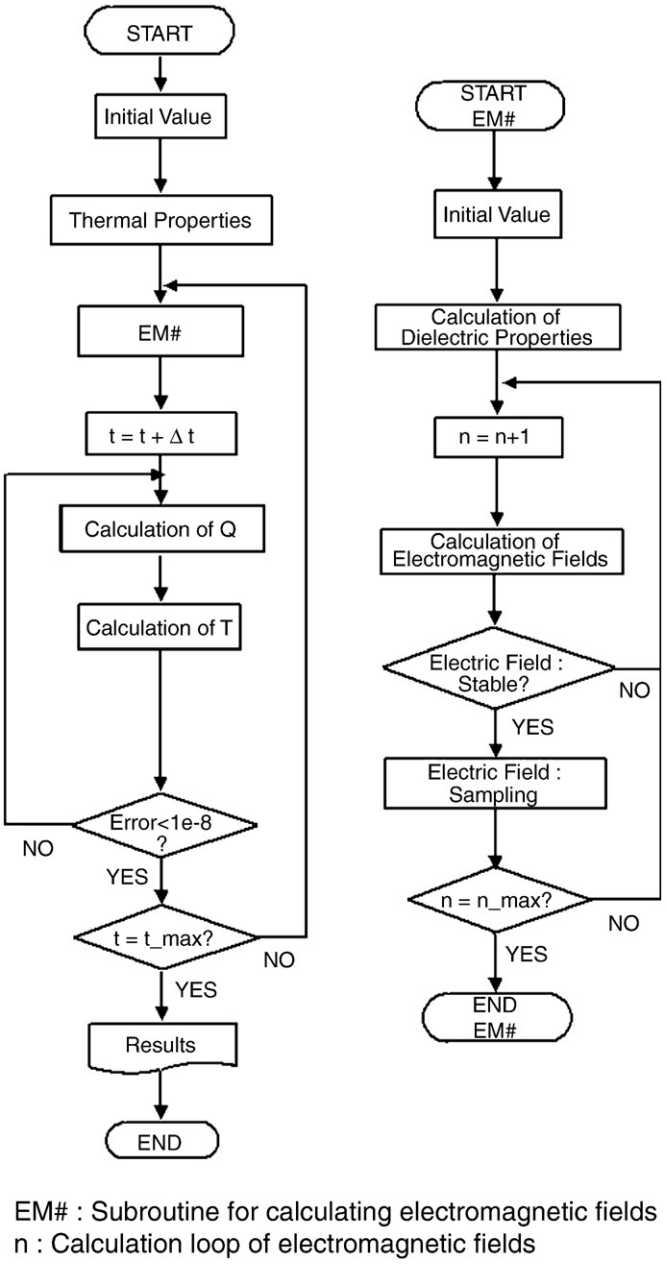

Fig. 5. Computational schemes.

without carbon black become lower more gradually than those of the NRc specimens with carbon black; while the loss tangent coefficient tanδ is strongly affected by carbon black. This is because natural rubber as received is often non-polar; therefore, by adding and integriding uniformly with carbon black, increasing the ability of natural rubber to polarize and/or its sensitivity to polarization under microwave irradiation. In other words, carbon black acts as an absorber material that culminates significantly to absorb microwave energy and thereby increases heat conversion [19]. Furthermore, the penetration depths as calculated in Eq. (3) have a tendency that is similar to that of dielectric properties.

A typical variation of dielectric properties versus the temperature change of the NRC-S2.5 (2.5 phr sulfur content) is shown in Fig. 6. It is found that the dielectric constant tends to be almost uniform with increasing temperatures, whereas the loss tangent coefficient increases quickly at a temperature range of not more than 45 °C and decreases subsequently thereafter up to 80 °C.

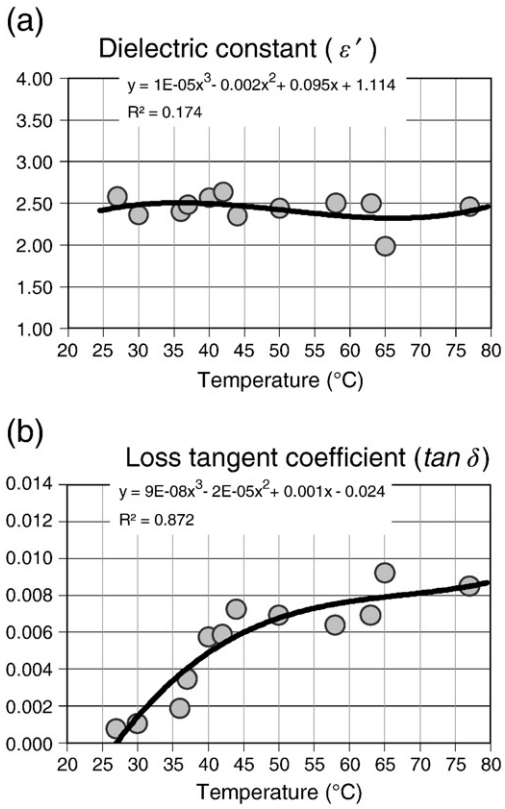

Fig. 6. The temperature dependence of the dielectric properties of the NR-S2.5 specimen: (a) dielectric constant and (b) loss tangent coefficient.

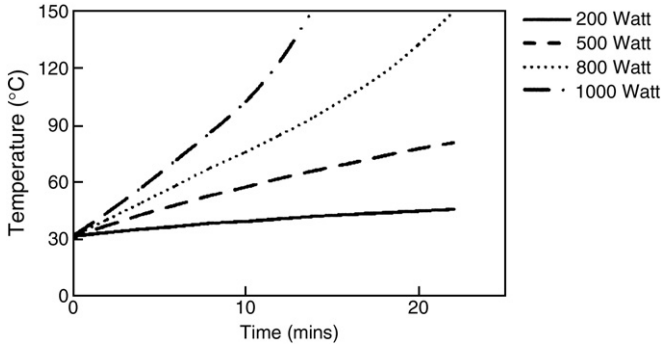

Fig. 7. Temperature rise within the NRc specimen as a function of time at various microwave powers.

4.2. Heating characteristics

Experiments using microwave energy to pre-cure NRc specimens are conducted. The effects of microwave power's input, specimen thicknesses, and vulcanized sulfur contents are discussed. Not only do the dielectric properties vary with temperature during the curing process, but the thermal properties of NRc specimens are directly taken from our experiment and literatures [18,19]. In the microwave industry, only a few frequencies are available. Currently, the operating frequency of 2.45 GHz has been selected.

In theoretical analysis, a dry basis density of 1100 kg/m^3, a moisture content of 0.02% and an initial temperature of 25 °C are set as parameters for simulating the power distribution and temperature characteristics. Since the average moisture content of the rubber specimen is very low due to high-temperature grinding and the overall curing time is fast, the moisture content is specified as having a constant value throughout the microwave pre-curing procedure.

4.2.1. Effect of the input of microwave power

Fig. 7 shows the variation of temperature distribution inside an NRc specimen with a microwave power level during pre-curing. It is found that when the NRc specimen is subjected to increasing microwave power, its temperature rises; this is because high microwave power (electric field) can generate high local volumetric heat inside the specimen, as shown in Eq. (2). Typically, a profile temperature rise at a power input of 200 W occurs gradually in accord with the ambient temperature because of low microwave power and some heat loss. Meanwhile the microwave powers of 500 W, 800 W, and 1000 W effect sudden temperature increases as compared to the power of 200 W under similar conditions of heat loss.

In regard to the temperature distribution of the NRc specimen inside the wave, Fig. 8 shows a typical temperature distribution of NR-S2.5 at a microwave power of 1000 W along the *x*- and *z*-directions. Fig. 8a points out that the temperature increases more in the *x*-direction with longer application times. In addition, the middle location has the highest temperature level with a high power intensity, generating more heat than the other locations. Accordingly, in Fig. 8b, the highest temperature is located at 5.0 cm from the first contacting surface. This is because the thickness of the NRc specimen is lower than its penetration depth, which brings reflection of the microwave back to the specimen's bottom side. Consequently, the reflection and transmission components at this side contribute to the standing wave resonance inside the processed specimen and above a certain temperature can cause damage to the specimen.

Under consideration in the simulation results, the temperature rise during the microwave pre-curing of the NRc specimen are shown in Figs. 9 and 10. The curing conditions consist of microwave power input of 500 W and 1000 W and the input parameter values as given in Table 2. In Fig. 9, temperature distributions correspond to the electric field distribution in the specimen. This is because the electric field within the specimen attenuates owing to energy absorption, and thereafter either the absorbed energy converts to thermal energy or the temperature increases. Furthermore, it can be seen that the temperature distributions inside the specimen display a wavy behavior. This is because (1) the penetration depth of microwave drops immediately, and (2) the wavelength is short. As the reflected wave from the lower surface of the specimen is neglected, a weak resonance is formed within the specimen. Therefore, the microwave power absorbed decreases sharply to a small value along the propagating direction ($+z$). The maximum temperature within the rubber specimen is around 53 °C in the *z*-direction during the first 5 min of pre-curing.

In the case of a microwave power input of 1000 W, the predictions of temperature distributions as shown in Fig. 10 found a strong wavy behavior corresponds to a strong electric field. This is due to the fact that the electric field within the specimen attenuates on account of the energy absorbed and thenceforth the absorbed energy is converted to the thermal energy and consequently increases the specimen temperature. Moreover, temperature levels decay gradually with a strong wavy behavior along the propagation direction ($+z$) following the absorption of the microwave.

4.2.2. Effect of application time

Fig. 11 shows the temperature rise as a function of the application time of microwave energy. It can be observed from Fig. 7 that for the NRc specimen at a thickness of 3.0 cm and subjected to a power of 1000 W, the test results indicated that sulfur content has a little effect on temperature increases because apart from heat, which is generated by the electric field, the dielectric properties of the NRc specimen are essential parameters used to determine the ability to produce heat. In dielectric properties results, NRc specimens have similar loss tangent coefficient ($\tan\delta$) values, and that it can be confirmed that the

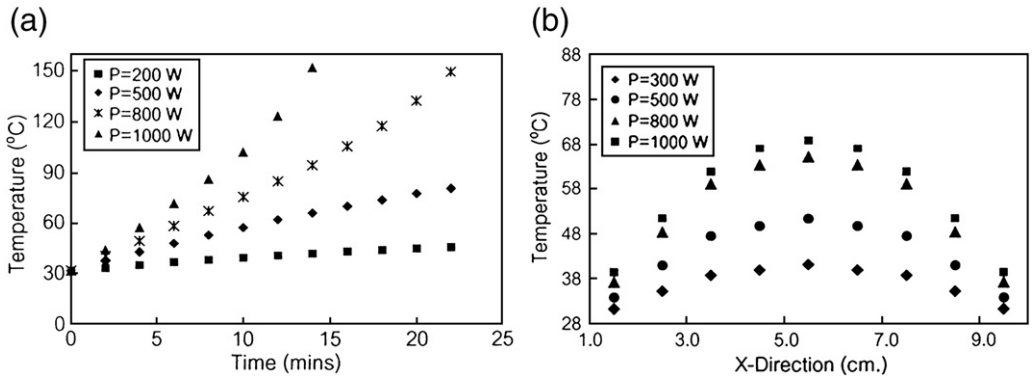

Fig. 8. Distributions of temperature within NR-S2.5 specimen as a function of (a) time at various microwave powers ($x = 5.5$ cm) and (b) distance at various microwave powers ($z = 0.5$ cm).

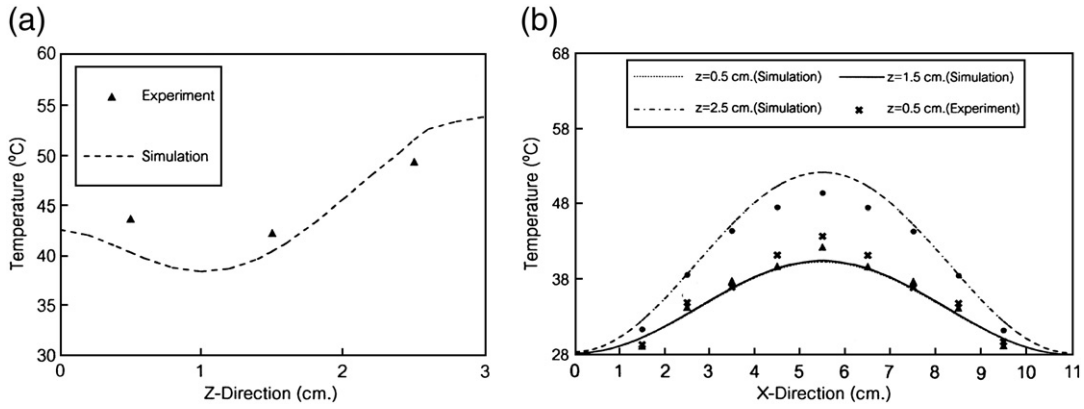

Fig. 9. Comparison of the distribution of temperature within the NRc specimen from simulation and experiment at a microwave power of 500 W as a function of (a) time ($x = 5.5$ cm) and (b) distance from the contacting surface ($z = 0.5$ and 1.5 cm).

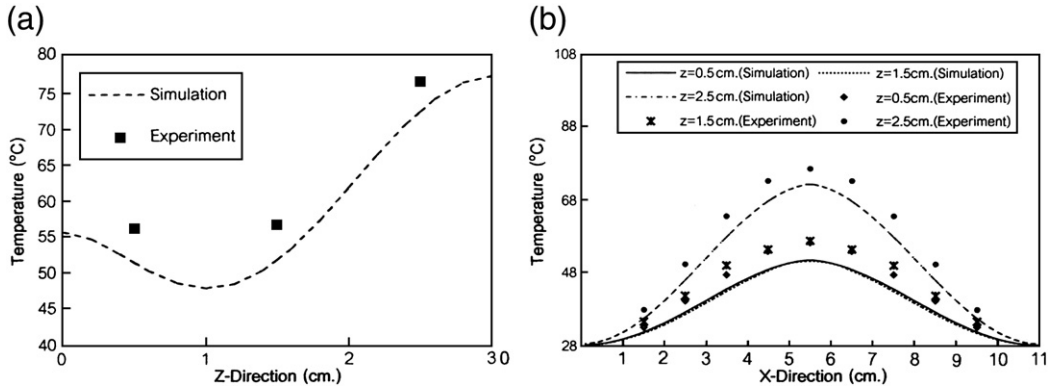

Fig. 10. Comparison of the distribution of temperature within the NRc specimen from simulation and experiment at a microwave power of 1000 W as a function of (a) time ($x = 5.5$ cm) and (b) distance from the contacting surface ($z = 0.5$ cm, 1.5 cm, and 2.0 cm).

Table 2
Parameter values used for simulation.

Parameters	Values	Units	References
Density (ρ)	1100	kg/m^3	Authors
Thermal conductivity (k)	0.13	W/m K	[20]
Heat capacity	2010	J/kg K	[20]
Relative dielectric constant(ε_r')	3.544	–	Authors
Relative loss factor (ε_r'')	0.0338	–	Authors

different sulfur contents affect heat generation due to the *d* polarity of the NRc specimen is improved.

4.2.3. Effect of simple thickness

Fig. 12 shows the temperature rise inside the NRc specimens during microwave pre-curing as a function of the application time at a microwave power of 1000 W and respective specimen thicknesses of 1.0 cm, 2.0 cm, and 3.0 cm. It can be observed that the rates of

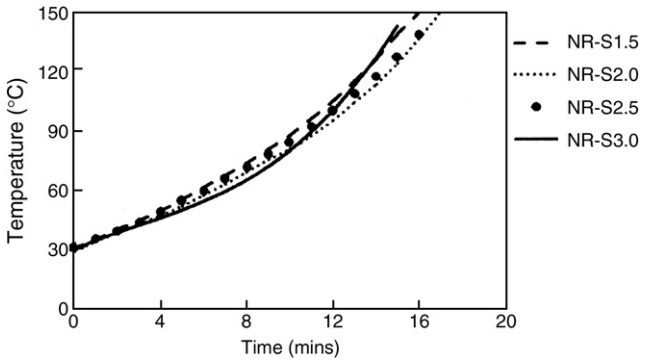

Fig. 11. Temperature rise within the NRc specimen as a function of application time at microwave power of 1000 W and varying proportions.

temperature rise are similar for all the thicknesses in the first 5 min of curing. After that, however, for the NRc specimens with 1.0 cm and 2.0 cm thicknesses to show a temperature increase takes more curing time than for the 3.0 cm to do so. This is because the thick specimens are more effective at storing heat than are thinner ones.

In order to understand the distribution of temperature inside the NRc specimen during microwave pre-curing, it is necessary to conduct a simulation analysis based on input data for electromagnetic and thermo-physical properties, as given in Table 2. The simulation results are displayed in Fig. 13, which corresponds to the initial temperature of 28 °C, a microwave power level of 1000 W, an application time of 5 min, and specimen thicknesses of 1.0 cm and 3.0 cm. Most importantly, temperature distribution inside the cured specimen depends to a great extent on the specimen's thickness. Further results indicate that microwave power absorbed and temperature distribution are at their highest values on the lower surface of the specimen. This is so not only because the NRc specimen has a penetration depth that is greater than its thickness (as shown in Table 3), but also because the wave length within the specimen is too long; this synergy, therefore, can cause most of the microwave energy to penetrate the specimen and reflect back to some parts. Consequently, the reflection and transmission components at a low interfacial surface contribute to the resonance of the standing wave inside the NRc specimen as shown by the microwave power absorbed in Fig. 13a and c and the temperature generation taking place at the lower surface of the specimen at high level has more than the upper or leading surface as shown in Fig. 13b and d.

4.3. Chemical characteristics: cross-linked content and its structure

Normally, the cross-linked contents of a microwave-cured NRc specimen depends on its sulfur content; that is, a high quantity of sulfur tends to increase cross-linked density, as shown in Fig. 14. It

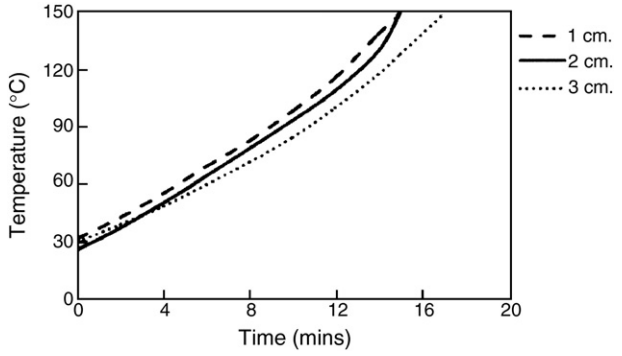

Fig. 12. Temperature rise within the NRc specimen as a function of application time at microwave power of 1000 W and varying specimen thicknesses.

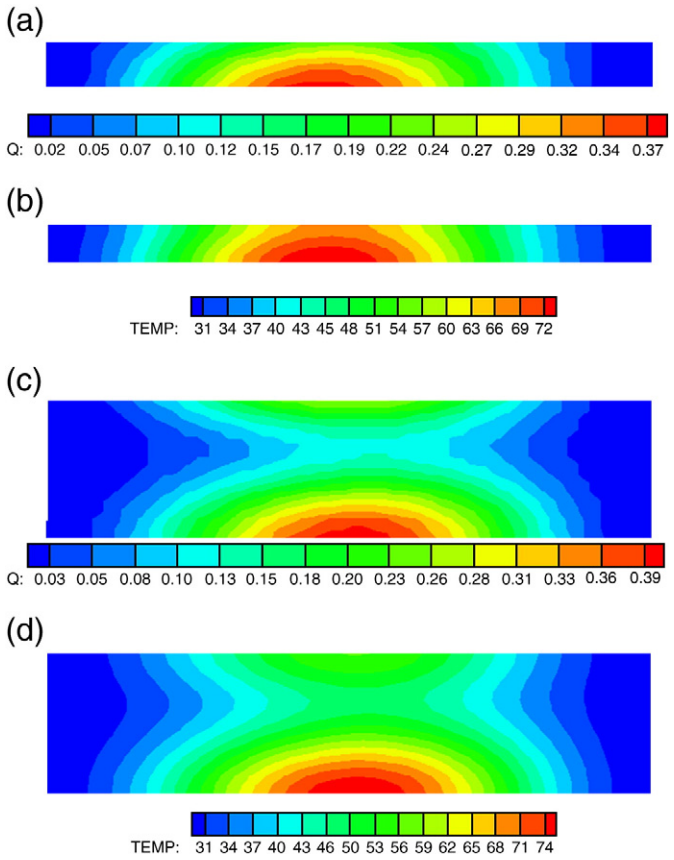

Fig. 13. Analytical results illustrate the microwave energy absorbed and the temperature distribution of the NRc specimen subjected to microwave pre-curing at a frequency of 2.45 GHz, power of 1000 W, and application time of 5 min: (a) microwave power absorbed at specimen thickness of 1.0 cm; (b) temperature distribution at specimen thickness of 1.0 cm; (c) microwave power absorbed at specimen thickness of 3.0 cm; and (d) temperature distribution at specimen thickness of 3.0 cm.

Table 3
Dielectric properties and penetration depth of NRc before pre-heating.

Mix symbol	Relative dielectric constant (ε_r')	Relative loss factor (ε_r'')($\times 10^{-3}$)	Loss tangent coefficient ($\tan\delta$)($\times 10^{-3}$)	Penetration depth (meter)
NR[a]-S1.5[b]	2.043	0.000002	0.000001	19468.91
NR-S2.0	2.161	0.000004	0.000002	9734.48
NR-S2.5	2.017	0.000009	0.000004	4326.39
NR-S3.0	2.273	0.000004	0.000002	9734.09
NRC[c]-S1.5	3.642	0.0287	0.007880	1.36
NRC-S2.0	3.439	0.0183	0.005321	2.13
NRC-S2.5	3.544	0.0338	0.009537	1.15
NRC-S3.0	3.366	0.0142	0.004219	2.74

[a] Natural rubber-compounding without carbon black.
[b] Sulfur content (part per hundred parts by dry basis weight).
[c] Natural rubber-compounding with carbon black.

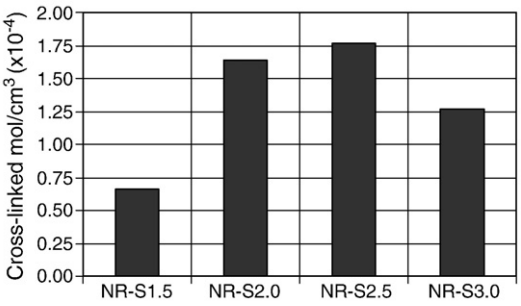

Fig. 14. Cross-linked contents of the NRc specimen after microwave pre-heating.

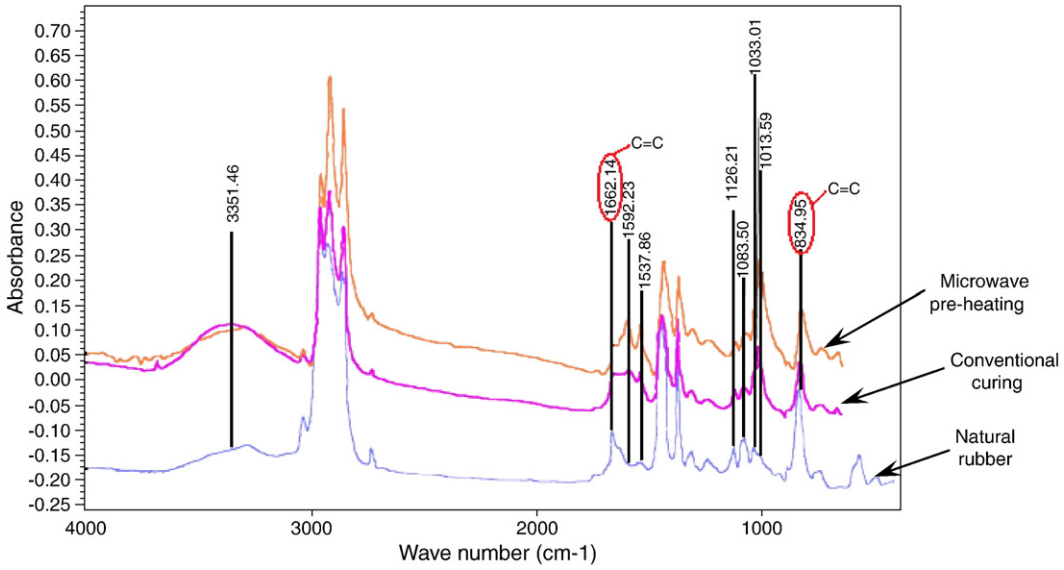

Fig. 15. Spectrum patterns of the Fourier Transform Infrared Spectroscopy (FTIR) of the NRc specimen after curing by conventional and microwave methods in comparison with natural rubber (STR 20).

can be seen that the NRc specimen with high sulfur content has high cross-linked density, while the NRC-S3.0 rubber specimen has a lower sulfur content than the NRC-S2.0 and NRC-S2.5 specimens. This is because large amounts of sulfur can induce a blooming formation, a phenomenon whereby liquid or solid material migrates to the surface of a rubber and changes the rubber's appearance. This is a different effect than that accruing from adding carbon black to the mix, which does not affect cross-linking, whereas sulfur is an important reactant in cross-linking formation. Therefore, in nature, before adding chemical compounding, the NRc specimen has two bonds that make it highly reactive when sulfur is added and microwave energy is applied. This means that heat generation inside the specimen takes place at the molecular level and dissipates outwards. In other words, this heating mechanism effects a uniform degradation of the rubber, such that bi-bonding becomes single-bonding or such that better cross-linking products result.

The Fourier Transform Infrared Spectrometer technique can be used to monitor product quality. The FTIR spectrums of natural rubber (STR 20) and the NRc specimen cured by conventional and microwave methods are shown in Fig. 15. It is found that as compared with natural rubber (STR 20), the NRc specimen's peak was at wavelength of 834 cm^{-1}, which indicates the C–C bonding of the isoprene; however, curing the specimen by conventional and microwave methods reduces this peak level and is directly related to the occurrence of cross-linking in the NRc specimen.

5. Conclusions

Both the experimental results and numerical analysis presented here identify and illustrate many important interactions that take place in the NRc specimen during pre-curing by means of microwave energy using a rectangular wave guide. The conclusions of this study can be clearly summarized thus:

(1) Microwave energy assisted the pre-curing of the NRc specimen and consequently produced partial cross-linking at a temperature below the actual vulcanizing process when sulfur content was added up to 2.5 parts per hundred parts by dry basis weight of the NRc specimen. Moreover, sulfur content had precious little effect on temperature rise, and the NRc specimen without carbon black absorbed microwave energy transferred less effectively than did the NRc specimen with carbon black.

(2) The results from a generalized mathematical model for predicting the temperature rise and distributions of the NRc specimen during microwave pre-curing accords with the experimentally obtained data.

Acknowledgment

The authors wish to acknowledge the Thailand Research Fund (TRF) for financial support.

References

[1] M. Abdulhadi, Temperature distribution inside a vibrating rubber cylinder, International Communications in Heat and Mass Transfer 13 (3) (1986) 357–365.
[2] N. Doo-ngam, et al., Microwave pre-heating of natural rubber using a rectangular wave guide (MODE: TE_{10}), Songklanakarin Journal Science and Technology 29 (6) (2007) 1599–1608.
[3] N. Sombatsompop, C. Kumnuantip, Comparison of physical and mechanical properties of NR/carbon black/reclaimed rubber blends vulcanized by conventional thermal and microwave irradiation methods, Journal of Applied Polymer Science 100 (6) (2006) 5039–5048.
[4] D. Martin, et al., Vulcanization of rubber mixtures by simultaneous electron beam and microwave radiation, Physics and Chemistry 65 (2002) 163–165.
[5] D. Bogdal, J. Pielichowski, Microwave assisted synthesis, crosslinking and processing of polymer materials, Journal AIChE Annual Meeting, conference proceedings, 2004, p. 1457.
[6] H. Chen, Simulation model for moving food packages in microwave heating processes using conformal FDTD method, Journal of Food Engineering 88 (3) (2008) 294–305.
[7] S. Vongpradubchai, P. Rattanadecho, The microwave processing of wood using a continuous microwave belt drier, Journal of Chemical Engineering and Processing: Process Intensification 48 (5) (2009) 997–1003.
[8] J. Dobozy, Method and apparatus for recovering elastomeric material, United States Patent 6 722 593 (2004).
[9] G.G. Wicks, R.L. Schulz, Clark, D.E., and Folz, D.C., Microwave treatment of vulcanization rubber, United States Patent 6 420 457 (2002).
[10] V. Bovtun, W. Stark, J. Kelm, V. Porokhonsky, Y. Yakimenko, Microwave dielectric properties of rubber compounds undergoing vulcanization, KGK-Kautschuk und Gummi Kunststoffe 54 (12) (2001) 673–678.
[11] D. Bogdal, P. Penczek, J. Pielichowski, A. Prociak, Microwave assisted synthesis, crosslinking and process of polymeric materials, Advances in Polymer Science 163 (2003) 193–263.
[12] L. Landini, S.G. Araújo, A.B. Lugão, H. Wiebeck, Preliminary analysis to BIIR recovery using the microwave process, European Polymer Journal 47 (2007) 2725–2731.
[13] C.Y. Khor, et al., Three-dimensional numerical and experimental investigations on polymer rheology in meso-scale injection molding, International Communications in Heat and Mass Transfer 37 (2) (2010) 131–139.
[14] P. Perre, W. Turner, Microwave drying of softwood in an oversized waveguide, Journal AIChE 43 (1997) 2579–2595.

[15] H. Zhao, I.W. Turner, The use of a coupled computational model for studying the microwave heating of wood, Applied Mathematical Modelling 24 (2000) 183–197.
[16] P. Rattanadecho, Influences of irradiation time, particle sizes and initial moisture content during microwave drying of multi-layered capillary porous materials, Journal ASME Heat Transfer 124 (1) (2002) 151–161.
[17] P. Rattanadecho, K. Aoki, M. Akahori, A numerical and experimental investigation of the modeling of microwave heating for liquid layers using a rectangular wave guide (effect of natural convention and dielectric properties), Applied Mathematical Modelling 26 (3) (2002) 449–472.
[18] T.C. Allen, B. Bryan, L. James, Characterization of polymer-filler interface in-irradiated silica-reinforces polysiloxane composites, Materials Research Society 629 (2003) FF5.14.1–FF5.14.5.
[19] L. Estel, A.C. Bonnet, M. Delmote, J.M. Cosmao, Kinetic analysis via microwave dielectric measurement, Chemical Engineering Research and Design 81 (A9) (2009) 1212–1216.
[20] P.S. Ghoshdastidar, Heat transfer, Oxford Express, 2004.